

ORIGINAL ARTICLE

# Chatter detection in milling process based on synchrosqueezing transform of sound signals

Hongrui Cao<sup>1</sup> · Yiting Yue<sup>1</sup> · Xuefeng Chen<sup>2</sup> · Xingwu Zhang<sup>2</sup>

Received: 30 July 2016 / Accepted: 19 October 2016

© Springer-Verlag London 2016

**Abstract** Chatter is a self-excited vibration between the workpiece and tool with negative effects. In this work, a chatter detection method is proposed based on synchrosqueezing transform (SST) of sound signals. Firstly, the SST is used to analyze the sound signals recorded with the microphone and a time-frequency representation is obtained. Then, filtering is conducted to remove the disturbance of tooth passing frequency and its harmonics in time-frequency domain. Next, singular value decomposition (SVD) method is employed to condense the TF matrix and the first-order singular value is calculated as the chatter indicator. Finally, chatter threshold is set based on  $3\sigma$  criterion for the detection of chatter occurrence. The proposed method is validated with cutting tests, and the results show that the method has great potential to be used for the online chatter detection of high-speed milling process.

**Keywords** Chatter detection · Synchrosqueezing transform · Singular value decomposition · Sound signals · Milling

## 1 Introduction

Chatter is the self-excited vibration between the workpiece and tool, which may cause poor surface quality, disproportionate tool wear, tool breakage, etc. It is significant to conduct

chatter detection and suppression/control to improve surface quality and avoid damages in machining process.

Appropriate selection of sensors can increase the sensitivity, accuracy, and robustness of chatter detection systems. Since the physical essence of chatter is vibration, the idea of using vibration signals for chatter detection and prediction [1–6] is clear. Moreover, regenerative chatter results in excessive machining forces [7–9] and subsequently increases the motor current/power [10–14], which can also be used for chatter monitoring. The sound or acoustic emission (AE) signals emerging from mechanical vibrations produced in the cutting zone can also be used to detect and control chatter occurrence. Due to the simple and non-contact measurement setup, the sound signal is easily collected and not intrusive in the milling process. In the past, various chatter detection techniques were reported based on sound signals [15–21]. Delio et al. [15] compared the microphone with other commonly used sensors (e.g., dynamometers, displacement probes, and accelerometers) and concluded that sound signals were the most appropriate for chatter detection in many instances. Altintas and Chan [16] conducted frequency spectrum analysis on sound signals and the maximum amplitude in the frequency spectrum was used as an indicator for chatter detection. The statistical variance of the once-per-revolution sound signal was calculated as a chatter indicator [17]. The time-based audio signal was analyzed off-line to identify chatter frequencies, and the sound map was built to obtain the stability lobe diagram [18]. Jin and Poudel [19] monitored the chatter vibration using the sound pressure signal in the micro milling process. Yang et al. [20] and Wan et al. [21] measured sound and cutting forces together with their frequency spectra for milling. Besides milling process, sound signals were also used for chatter detection in turning [22–24].

✉ Hongrui Cao  
chr@mail.xjtu.edu.cn

<sup>1</sup> Key Laboratory of Education Ministry for Modern Design and Rotor-Bearing System, Xi'an Jiaotong University, Xi'an 710049, China

<sup>2</sup> State Key Laboratory for Manufacturing Systems Engineering, Xi'an Jiaotong University, Xi'an 710049, China

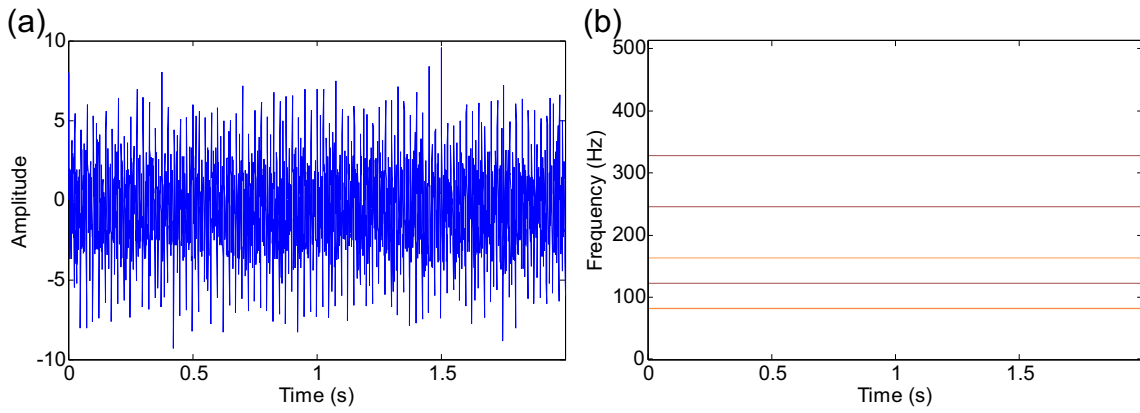


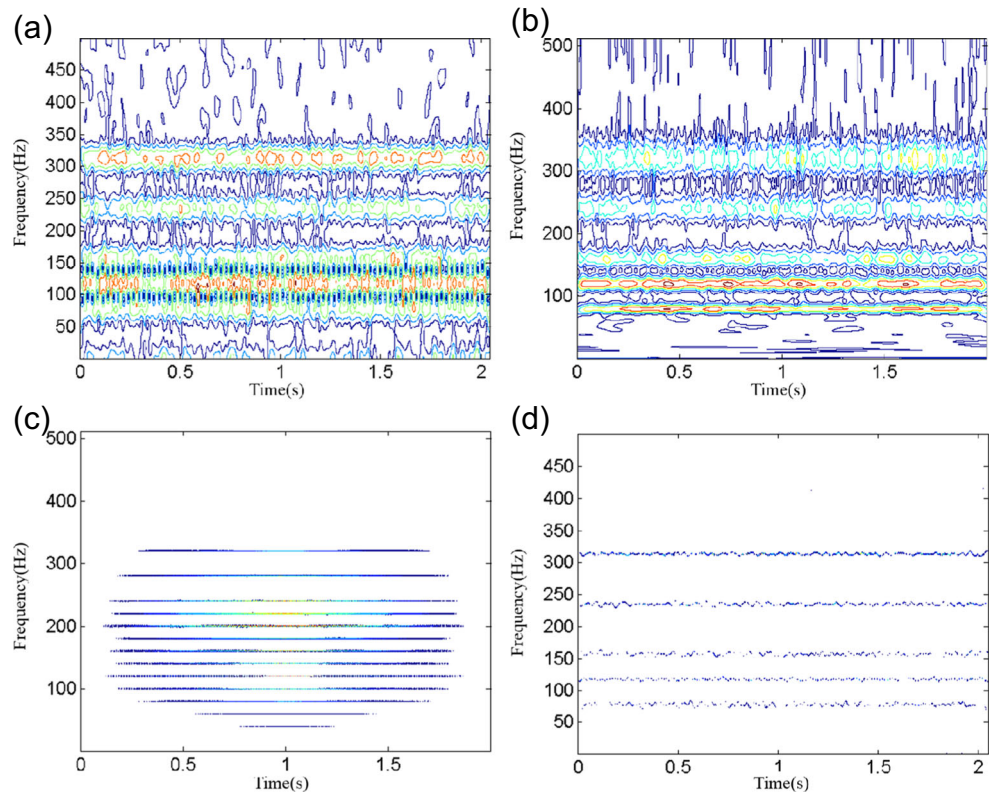
**Fig. 1** The simulated signal  $s(t)$ . **a** The waveform in time domain. **b** The TF representation

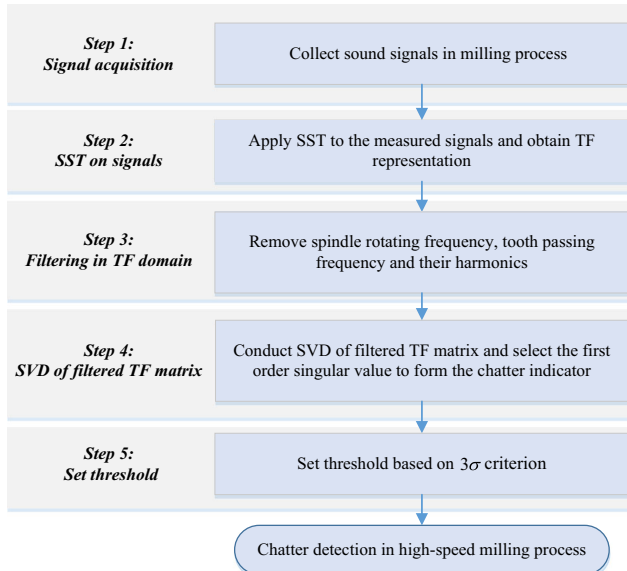
However, sound signals can be easily distorted by noises and heavily dependent on process parameters; advanced signal processing techniques are required. The signal processing methods used in chatter detection can be primarily classified as three categories: time domain analysis [14, 25, 26], frequency domain analysis [27–31], and time-frequency (TF) domain analysis [32–37]. Due to the nonstationary properties of sound signals in machining processes, the TF representation methods attract more attentions. The information in both time and frequency domains can be combined together to achieve better results. In linear TF representations, such as short-time Fourier transform (STFT) and wavelet transform,

the time and frequency resolutions are limited by Heisenberg uncertainty principle. Meanwhile, in quadratic TF representations such as Wigner–Ville distribution (WVD), the cross terms between multi-components reduce the readability of the TF distribution. Aiming at high resolution in TF plane, Daubechies et al. [38] developed the synchrosqueezing transform (SST). Subsequently, the SST method was improved and applied in many fields, such as biomedical sciences [39], geological climate [40], seismic signal analysis [41], and mechanical fault diagnosis [42–44].

SST is a powerful time-frequency analysis tool with high resolution. With the rearrangement along the frequency

**Fig. 2** The comparison of four TF analysis methods. **a** STFT. **b** CWT. **c** WVD. **d** SST

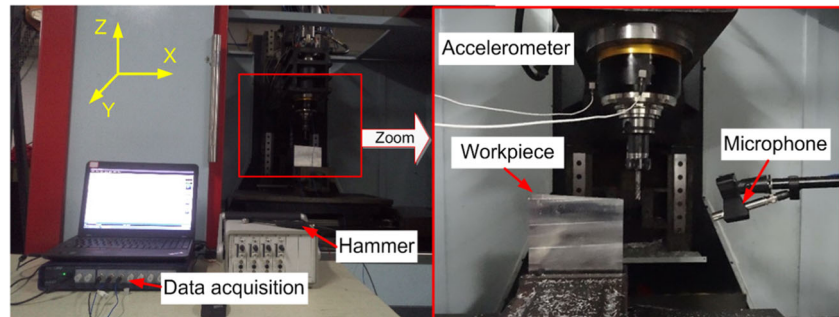


**Fig. 3** The flowchart of the proposed chatter detection method

direction, the obtained TF representation has higher energy aggregation, which has great potential to reflect the change of the energy distribution when chatter occurs. In this work, the SST is used for chatter detection for the first time. Section 2 briefly overviews the basic principle of SST, and the chatter detection method is proposed in Section 3. Section 4 presents experimental verification and discussions, and conclusions are given in Section 5.

## 2 Brief overview of synchrosqueezing transform

The “Synchronization” means that there is no reassigned movement for each TF point on time axis while the “squeezing” refers to reassigned movement on frequency axis. The so-called synchrosqueezing transform is to get the more ideal TF distribution by improving the beforehand TF distribution based on STFT, continuous wavelet transform (CWT), etc. In this work, the SST is based on STFT and the principle and computational procedure are presented as follows [45].

**Fig. 4** The experimental setup

For a signal  $x(t)$ , its STFT is defined as,

$$S_x(\mu, \xi) = \int_{-\infty}^{+\infty} x(t)g(t-\mu)e^{-i\xi(t-\mu)}dt \quad (1)$$

where  $g(t)$  is a Gaussian window function,  $\mu$  is the time-shifting variable, and  $\xi$  is the frequency shifting variable of  $g(t)$ .

According to the definition in Eq.(1) and the Plancherel theorem, the TF representation  $S_x(\mu, \xi)$  of a purely harmonic signal, namely,  $x(t)=A \cos (\omega_0 t)=A \cos (2\pi f_0 t)$ , can be presented as,

$$\begin{aligned} S_x(\mu, \xi) &= \frac{1}{2\pi} \int_{-\infty}^{+\infty} \hat{x}(\omega)\hat{g}(\omega-\xi)e^{i\omega\mu}d\omega \\ &= A \int_{-\infty}^{+\infty} \delta(\xi-\omega_0)\hat{g}(\omega-\xi)e^{i\omega\mu}d\omega \\ &= A\hat{g}(\omega_0-\xi)e^{i\omega_0\mu} \end{aligned} \quad (2)$$

where  $\hat{x}(\omega)$  and  $\hat{g}(\omega-\xi)$  are the Fourier transform of  $x(t)$  and  $g(t-\mu)$ , respectively. Then, the time-shift partial derivative of  $S_x(\mu, \xi)$  is calculated as,

$$\partial_\mu S_x(\mu, \xi) = A\hat{g}(\omega_0-\xi)e^{i\omega_0\mu} \cdot i\omega_0 = i\omega_0 S_x(\mu, \xi) \quad (3)$$

where  $\partial_\mu S_x(\mu, \xi) = \partial S_x(\mu, \xi)/\partial\mu$  means the partial derivative of the time-shifting variable. If  $S_x(\mu, \xi) \neq 0$ , then instantaneous frequency (IF) can be obtained,

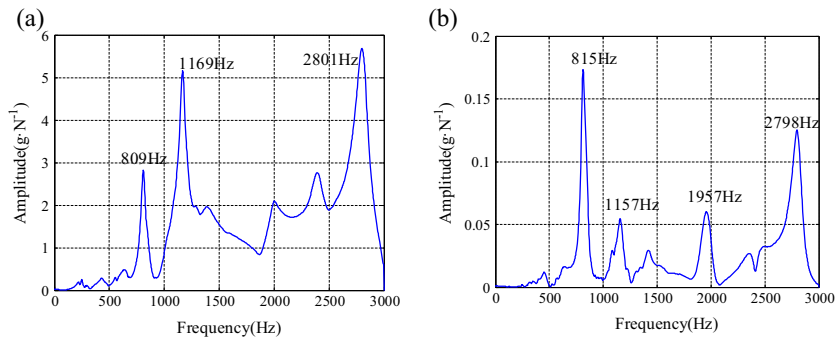
$$\tilde{\omega}_x(\mu, \xi) = \omega_0 = \frac{\partial_\mu S_x(\mu, \xi)}{iS_x(\mu, \xi)} \quad (4)$$

According to the reconstitution nature of STFT and the fact that IF estimation operator  $\tilde{\omega}_x(\mu, \xi)$  can reflect frequency information, the rearrangement formula is given as,

$$T_{x,S}(\mu, \omega) = \int S_x(\mu, \xi) \delta(\omega - \tilde{\omega}_x(\mu, \xi)) d\xi \quad (5)$$

From the analysis above, the algorithm of SST based on STFT can be summed up as following three steps. The first step is to calculate the TF representation  $S_x(\mu, \xi)$  with STFT. Then, the IF estimation operator  $\tilde{\omega}_x(\mu, \xi)$  is obtained

**Fig. 5** FRFs of the STT system. **a** X direction. **b** Y direction



according to Eq. (4). The last step is to get new TF distribution  $T_{x,S}(\mu, \omega)$  by rearranging  $S_x(\mu, \xi)$ .

The superiority of the SST is demonstrated with a simulated signal  $s(t)$ , which consists of five sinusoid components and Gaussian white noise. The waveform and TF representation of  $s(t)$  are shown in Fig. 1.

$$\begin{aligned} s(t) = & 1.5\sin(2\pi \times 80t) + 1.5\sin(2\pi \times 160t) \\ & + 1.5\sin(2\pi \times 240t) + 2\sin(2\pi \times 320t) \\ & + 2\sin(2\pi \times 120t) + N(t) \end{aligned}$$

The simulated signal is analyzed by STFT, CWT, WVD, and SST, respectively, and the results of TF representations are shown in Fig. 2. Since the width of the window function is same in the whole frequency range, STFT has a fixed resolution. CWT gives acceptable resolution in low-frequency area (less than 100 Hz), but poor resolution in high-frequency area. As for WVD, the frequency resolution is high, but the cross terms between frequency components are very large. From the results, it can be seen that only SST can separate the five sinusoid components clearly with high-frequency resolution.

### 3 The proposed chatter detection method

The sounds emerging from mechanical vibrations produced in the cutting zone can be used to detect chatter occurrence.

When chatter occurs, the amplitude increases in time domain, meanwhile, some new frequency components named chatter frequencies arise in addition to spindle rotating frequency, tooth passing frequency, and their harmonics. It is very natural to conduct analysis in time-frequency domain for chatter detection. Figure 3 shows the flowchart of the proposed chatter detection method.

#### Step 1. Signal acquisition

The sound signal is measured with microphones in real-time.

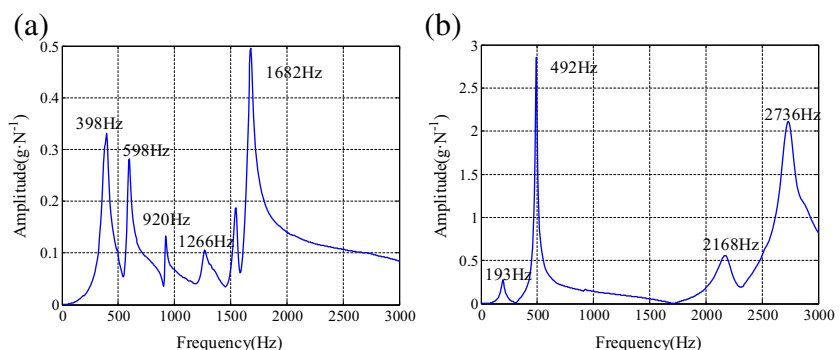
#### Step 2. SST on measured signals

The sound signal with a length of  $N$  is processed with SST, and a TF matrix  $\mathbf{S}_0$  with  $M$  rows and  $N$  columns is obtained to represent the TF representation.

#### Step 3. Filtering in TF domain

The spindle rotating frequency, tooth passing frequency, and their harmonics exist in the whole cutting process (stable or chatter), whose amplitudes are closely related with cutting parameters. It is necessary to discard these frequency components to highlight the chatter information. Instead of filtering in frequency domain, we simply remove these frequency components in the TF matrix. The new TF matrix after filtering is denoted as  $\mathbf{S}_1$ .

**Fig. 6** FRFs of the workpiece. **a** X direction. **b** Y direction



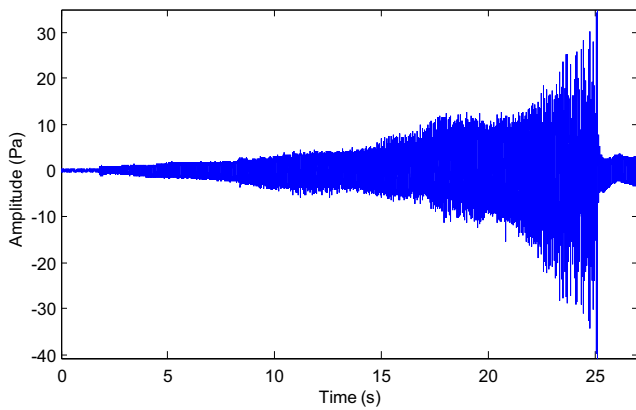


**Fig. 7** The sound signal in the whole machining process of test I

#### Step 4. Singular value decomposition (SVD) of filtered TF matrix

The TF representation can reveal the chatter information in both time and frequency domain, but it is not convenient to use TF representation for online chatter detection. The SVD is applied to condense the TF matrix  $\mathbf{S}_1$  into one-dimensional time series.

**Fig. 8** The TF representation of test I. **a** 2-dimensional. **b** 3-dimensional

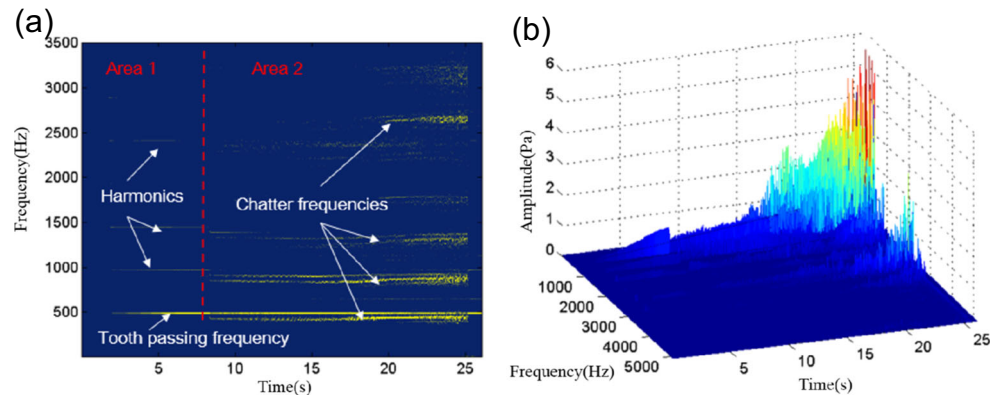
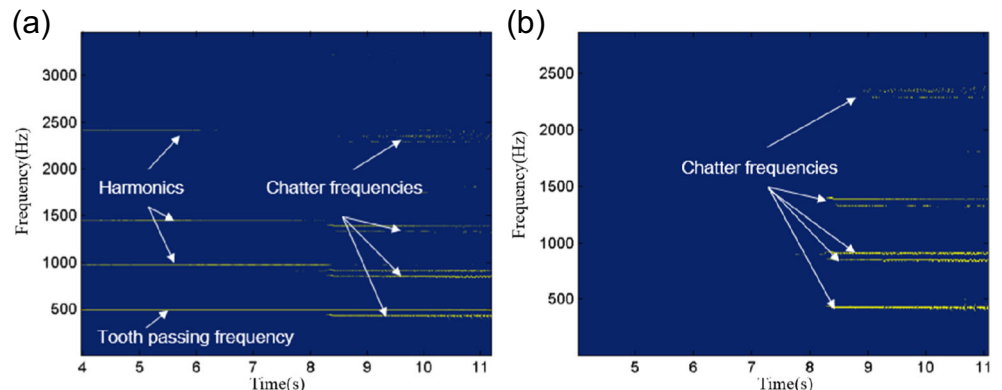


**Fig. 9** The partial TF representations in time interval (4–11 s) of test I. **a** Before filtering. **b** After filtering



Firstly, the data at time  $t_i = i\Delta t$  and  $t_{i-1}, t_{i-2}, \dots, t_{i-K+1}$  are extracted from  $\mathbf{S}_1$  to form a  $M \times K$  matrix  $\mathbf{A}_i$ :

$$\mathbf{A}_i[f, k\Delta t] = \mathbf{S}_1[f, (i-(K-k))\Delta t] \quad (6)$$

where  $k=0, 1, \dots, N-1$ ,  $f$  is the frequency, and  $\Delta t$  is time interval.

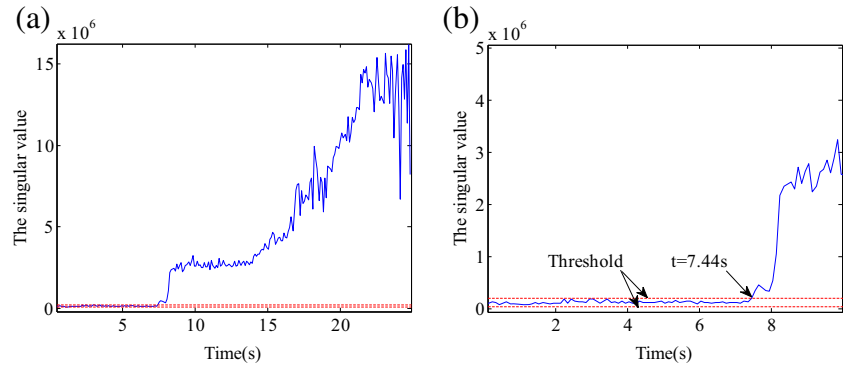
The SVD is conducted on matrix  $\mathbf{A}_i$ , namely,

$$\mathbf{A}_i = \mathbf{U}_i \mathbf{D}_i \mathbf{V}_i^T \quad (7)$$

where  $\mathbf{U}_i$  is  $M \times M$  left singular matrix,  $\mathbf{V}_i$  is  $K \times K$  right singular matrix, respectively, and  $\mathbf{U}_i \mathbf{U}_i^T = \mathbf{I}$ ,  $\mathbf{V}_i \mathbf{V}_i^T = \mathbf{I}$ .  $\mathbf{D}_i$  is  $M \times K$  diagonal matrix, whose diagonal elements  $d_1^i, d_2^i, \dots, d_p^i$  ( $d_1^i \geq d_2^i \geq \dots \geq d_p^i$ ,  $p = \min(M, K)$ )  $d_1^i, d_2^i, \dots, d_p^i$ ,  $(d_1^i \geq d_2^i \geq \dots \geq d_p^i, p = \min(M, K))$  are the singular values of  $\mathbf{A}_i$ . The first-order singular value  $d_1^i$  is the chatter indicator at time  $t_i$ . For the time after  $t_i$  ( $t_{i+1}, t_{i+2}, \dots, t_N$ ), we can use the same method to calculate the first-order singular values and form the vector of chatter indicator,

$$\mathbf{d}_1 = [d_1^i, d_1^{i+1}, \dots, d_1^N] \quad (8)$$

**Fig. 10** The first-order singular value of test I. **a** The whole time history. **b** The zoomed time interval



The vector  $d_1$  is the condensed information of TF matrix, representing the changes in TF representation.

#### Step 5. Set threshold

The threshold for chatter detection is set based on  $3\sigma$  criterion. Since the  $3\sigma$  criterion is based on the assumption of norm distribution, Lilliefors test is used to examine whether the chatter indicator  $d_1$  in stable cutting state meets the norm distribution assumption. Let  $\mu$  be the mean value of the chatter indicator  $d_1$  in stable milling state and  $\sigma$  as its standard deviation. Given chatter indicator  $d_1^i$ , if  $|d_1^i - \mu| \leq 3\sigma$ , the cutting state is stable, otherwise, chatter occurs.

## 4 Experiment and results

High-speed milling tests were carried out on three-axis high-speed CNC machine tools, as shown in Fig. 4. A carbide end mill cutter of three flutes was used to machine a thin-walled aluminum alloy workpiece of 7075 aluminum. The workpiece was designed as right trapezoid, which can make the axial

depth of cut continuously increase from 0 to 10 mm. The feed rate was set as 400 mm/min, while the spindle speed was set as 9600 r/min in test I and as 10,200 r/min in test II. The sound signals were measured by a MPA201 microphone, with the sampling frequency of 10,240 Hz.

### 4.1 Frequency response function (FRF) test

When chatter occurs and is not yet fully developed, the major chatter frequencies locate close to the low-order natural frequencies of the spindle-toolholder-tool (STT) or workpiece [46]. Hammer tests were carried out to obtain the FRFs, and then the possible chatter frequencies can be estimated roughly. In this way, we can determine whether the vibration signals come from chatter or forced vibration. The hammer Kistler 9722 (Fig. 4) was used to excite the tool tip and workpiece, and accelerometers were used to measure vibration responses of the STT and workpiece with the sampling frequency of 6000 Hz.

The FRFs of the STT system is shown in Fig. 5. It can be found that the low-order natural frequencies of the STT system are 809 and 1169 Hz in X direction, while 815 and 1157 Hz in Y direction. The FRF of the workpiece is shown in Fig. 6. The low-order resonant frequencies of the workpiece are 398, 598, 920, and 1682 Hz in X direction, while 193 and 492 Hz in Y direction. Due to the fact that the chatter frequencies are close to the low-order natural frequencies of the STT or workpiece, the frequency band ranging in 300–1700 Hz is selected as the chatter frequency band.

### 4.2 Results and discussions

The measured sound signal in test I is shown in Fig. 7. The entry time of the cutter into the workpiece is 1.8 s, and then the amplitude slowly increases with the axial depth of cut. At 25.5 s, the cutter exited from the workpiece. Since the amplitude of sound signals increases with axial depth of cut, even in

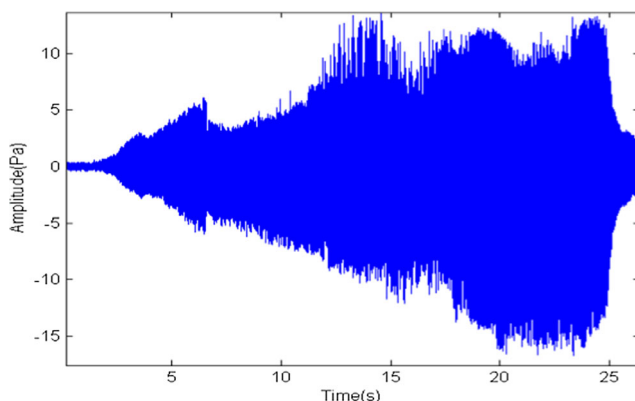
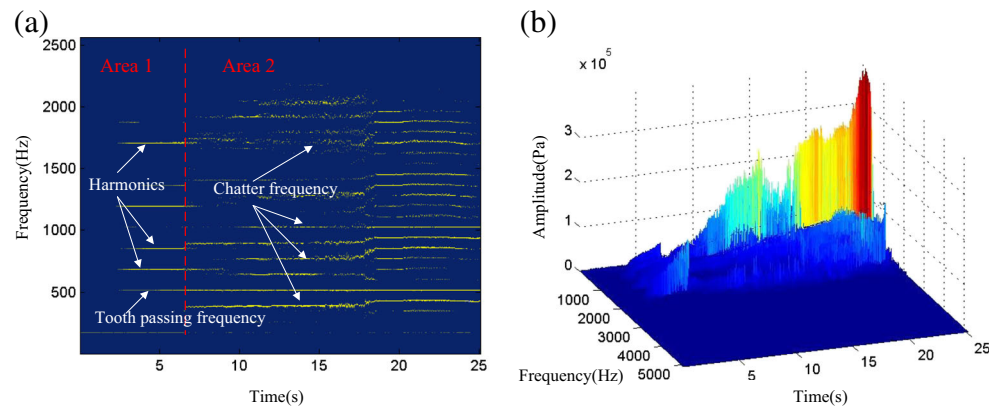


**Fig. 11** The sound signal in the whole machining process of test II

**Fig. 12** The TF representation of test II. **a** 2-dimensional. **b** 3-dimensional



stable cutting, it is difficult to distinguish whether the increase is caused by axial depth of cut or chatter.

The sound signal was analyzed by SST to get the TF representations, as shown in Fig. 8. In Fig. 8a, the TF representation can be divided into two areas by the red dotted line. In the area 1, the TF plane is dominated by tooth passing frequency (480 Hz) and its harmonics, indicating that the milling process is stable. In the area 2, some new frequency components appear which are close to the natural frequencies of the STT/workpiece system, indicating chatter occurs. From Fig. 8b, the amplitude corresponding to chatter frequencies increases with the axial depth of cut, which means the chatter becomes more and more severe.

From the TF representation, tooth passing frequency and its harmonics exist in the whole TF representation. In order to highlight the chatter frequencies, filtering is carried out in TF domain. Figure 9 shows the partial TF representations before and after filtering in time interval (4–11 s). It can be seen that the chatter frequencies become clear at around 8 s.

However, it is not convenient to identify the exact time of chatter occurrence from the TF representation. The SVD is applied to condense the TF matrix into one-dimensional time series. The first-order singular value was calculated and shown in Fig. 10. The overall trend of the singular value keeps increasing in the whole time history. In order to identify chatter automatically, the threshold based on  $3\sigma$  criterion is applied. The Lilliefors test is used to verify that the singular value in stable cutting state obeys the normal distribution. Before 7.44 s, the singular value curve changes smoothly

and the amplitude is very small, which is consistent with the stable milling process state. After 7.44 s, the singular value exceeds the threshold, indicating the chatter occurs. At around 8 s, the singular value increases suddenly, which denotes that the chatter is growing rapidly. Thus, the singular value can be used for online chatter detection.

In the test II, the spindle speed was increased up to 10,200 r/min. The sound signal in the whole machining process of test II is shown in Fig. 11. The entry time of the cutter into the workpiece is 1.8 s and the finished time is 25.5 s.

In the same way, the sound signals were analyzed by SST to get the TF representations in Fig. 12a. The rotating frequency is 170 Hz, and the tooth passing frequency is 510 Hz correspondingly. The milling process changed from stable to chatter, which can be proved by the appeared chatter frequencies in area 2. As the axial depth of cut increases, the energy at chatter frequencies increased as well (Fig. 12b).

In order to highlight the chatter frequencies, filtering was carried out in TF domain by eliminating the interference of tooth passing frequency and its harmonics. Figure 13 shows the partial TF representations before and after filtering in time interval (2–12 s). After filtering, it can be found that the chatter frequencies become clear at around 6.5 s.

In order to identify the exact time of chatter occurrence from the TF representation, the SVD was applied to condense the TF matrixes of test, then the first-order singular values were calculated. Similarly, the threshold based on  $3\sigma$  criterion was applied to identify chatter automatically and the results

**Fig. 13** The partial TF representations in time interval (2–12 s) of test II. **a** Before filtering. **b** After filtering

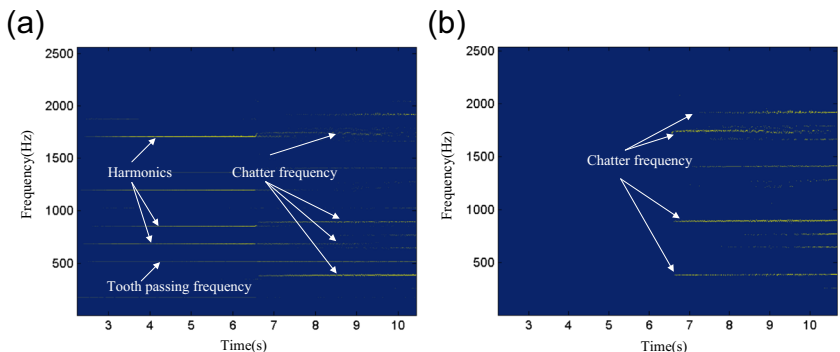
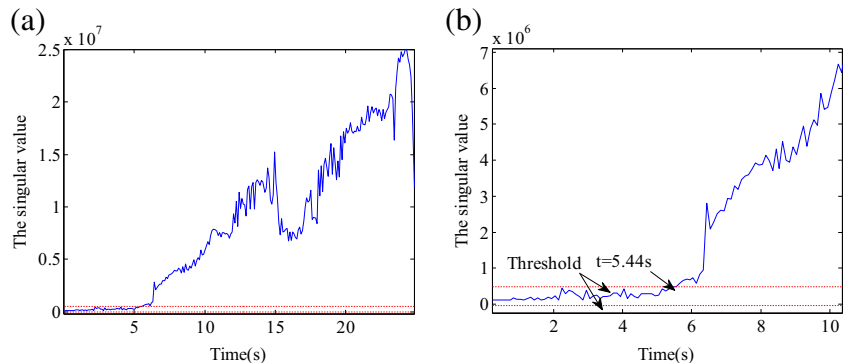


**Fig. 14** The first-order singular value of test II. **a** The whole time history. **b** The zoomed time interval



are shown in Fig. 14. The first-order singular value exceeds the threshold value at 5.44 s in test II, indicating the chatter occurs. After a short period of time (about 1 s), the singular value increases suddenly, which means that the chatter is becoming more serious.

## 5 Conclusions

A new chatter detection method based on the TF analysis method was presented in this study. The TF representation generated by SST can reflect the change of measured signals in time-frequency domain, which is superior to analysis methods in pure time or frequency domain. A filter in TF domain was applied to remove rotation frequency, tooth passing frequency and their harmonics, and hence chatter frequencies were highlighted without the change of amplitude and phase. In order to reflect the change of TF representation conveniently and quantitatively, SVD was used to condense the TF matrix and the first-order singular value was selected as the chatter indicator. Finally, the threshold method based on  $3\sigma$  criterion was utilized to detect chatter automatically. The high-speed milling experiments were carried out to verify the proposed method. The test results proved that the method can detect chatter before it is growing rapidly.

**Acknowledgements** The authors would like to acknowledge the support of the National Natural Science Foundation of China (No. 51575423, 51421004), Shaanxi Science and Technology Research Project (2014KJXX-33), and Fundamental Research Funds for the Central University.

## References

- Pérez-Canales D, Vela-Martínez L, Carlos Jáuregui-Correa J, Alvarez-Ramirez J (2012) Analysis of the entropy randomness index for machining chatter detection. *Int J Mach Tools Manuf* 62: 39–45
- Shao Y, Deng X, Yuan Y, Mechefske CK, Chen Z (2014) Characteristic recognition of chatter mark vibration in a rolling mill based on the non-dimensional parameters of the vibration signal. *J Mech Sci Technol* 28(6):2075–2080
- Lamraoui M, Thomas M, El Badaoui M (2014) Cyclostationarity approach for monitoring chatter and tool wear in high speed milling. *Mech Syst Signal Process* 44(1–2):177–198
- Wan M, Wang Y-T, Zhang W-H, Yang Y, Dang J-W (2011) Prediction of chatter stability for multiple-delay milling system under different cutting force models. *Int J Mach Tools Manuf* 51(4): 281–295
- Wan M, Ma Y-C, Feng J, Zhang W-H (2016) Study of static and dynamic ploughing mechanisms by establishing generalized model with static milling forces. *Int J Mech Sci* 114:120–131
- Wan M, Ma Y-C, Zhang W-H, Yang Y (2015) Study on the construction mechanism of stability lobes in milling process with multiple modes. *Int J Adv Manuf Technol* 79(1–4):589–603
- Huang P, Li J, Sun J, Zhou J (2012) Vibration analysis in milling titanium alloy based on signal processing of cutting force. *Int J Adv Manuf Technol* 64(5–8):613–621
- Tangjitscharoen S, Saksri T, Ratanakuakangwan S (2013) Advance in chatter detection in ball end milling process by utilizing wavelet transform. *J Intell Manuf* 26(3):485–499
- Lamraoui M, Thomas M, El Badaoui M, Girardin F (2014) Indicators for monitoring chatter in milling based on instantaneous angular speeds. *Mech Syst Signal Process* 44(1–2):72–85
- Kwak J-S, Ha M-K (2004) Neural network approach for diagnosis of grinding operation by acoustic emission and power signals. *J Mater Process Tech* 147(1):65–71
- Soliman E, Ismail F (1997) Chatter detection by monitoring spindle drive current. *Int J Adv Manuf Technol* 13(1):27–34
- Liu H, Chen Q, Li B, Mao X, Mao K, Peng F (2011) On-line chatter detection using servo motor current signal in turning. *Sci China Tech Sci* 54(12):3119–3129
- Zhigang Y, Hongqi L, Bin L, Xiaolong L 2011 Recognition of chatter in boring operations using spindle motor current. In, IEEE, pp 2158–2161
- Lamraoui M, El Badaoui M, Guillet F (2015) Chatter detection in CNC milling processes based on Wiener-SVM approach and using only motor current signals. *Vibration Engineering and Technology of Machinery* 23:567–578
- Delio T, Tlusty J, Smith S (1992) Use of audio signals for chatter detection and control. *ASME J Eng Ind* 114(2):146–157
- Altintas Y, Chan PK (1992) In-process detection and suppression of chatter in milling. *Int J Mach Tools Manuf* 32(3):329–347
- Schmitz TL, Medicus K, Dutterer B (2006) Exploring once-per-revolution audio signal variance as a chatter indicator. *Mech Sci Technol* 6(2):215–233
- Quintana G, Ciurana J, Ferrer I, Rodríguez CA (2009) Sound mapping for identification of stability lobe diagrams in milling processes. *Int J Mach Tools Manuf* 49(3–4):203–211
- Jin X, Poudel A (2015) Experimental study on high frequency chatter attenuation in 2-D vibration assisted micro milling process. *J Vibroeng* 17(6):2743–2754

20. Yang Y, Zhang W-H, Ma Y-C, Wan M (2016) Chatter prediction for the peripheral milling of thin-walled workpieces with curved surfaces. *Int J Mach Tools Manuf* 109:36–48
21. Wan M, Altintas Y (2014) Mechanics and dynamics of thread milling process. *Int J Mach Tools Manuf* 87:16–26
22. Yu SD, Shah V (2008) Theoretical and experimental studies of chatter in turning for uniform and stepped workpieces. *J Vib Acoust* 130(6):061005
23. Nair U, Krishna BM, Namboothiri VNN, Nampoori VPN (2010) Permutation entropy based real-time chatter detection using audio signal in turning process. *Int J Adv Manuf Technol* 46(1–4):61–68
24. Hynynen KM, Ratava J, Lindh T, Rikkonen M, Ryynänen V, Lohntander M, Varis J (2014) Chatter detection in turning processes using coherence of acceleration and audio signals. *J Manuf Sci Eng* 136(4):044503
25. Lamraoui M, Barakat M, Thomas M, Badaoui ME (2013) Chatter detection in milling machines by neural network classification and feature selection. *J Vib Control* 21(7):1251–1266
26. Du R, Elbestawi MA, Ullagaddi BC (1992) Chatter detection in milling based on the probability distribution of cutting force signal. *Mech Syst Signal Process* 6(4):345–362
27. Li XQ, Wong YS, Nee AYC (1998) A comprehensive identification of tool failure and chatter using a parallel multi-ART2 neural network. *J Manuf Sci Eng* 120(2):433–442
28. Tangjitsitcharoen S (2009) In-process monitoring and detection of chip formation and chatter for CNC turning. *J Mater Process Tech* 209(10):4682–4688
29. Liang M, Yeap T, Hermansyah A (2004) A fuzzy system for chatter suppression in end milling. *P I Mech Eng B-J Eng* 218(4):403–417
30. Li XQ, Wong YS, Nee AYC (1997) Tool wear and chatter detection using the coherence function of two crossed accelerations. *Int J Mach Tools Manuf* 37(4):425–435
31. Cao H, Zhang X, Chen X (2017) The concept and progress of intelligent spindles: a review. *Int J Machine Tools Manuf* 112: 21–52
32. Shih-Ming W, Ming-Je L, Sheng-Yu L, Hung-Wei L (2007) Application of wavelet transform on diagnosis and prediction of milling chatter. *Chin J Mech Eng-En* 20 (3):67–70
33. Chin DH, Yoon MC (2005) Cutting force monitoring in the end milling operation for chatter detection. *P I Mech Eng B-J Eng* 219(6):455–465
34. Yao Z, Mei D, Chen Z (2010) On-line chatter detection and identification based on wavelet and support vector machine. *J Mater Process Tech* 210(5):713–719
35. Cao H, Lei Y, He Z (2013) Chatter identification in end milling process using wavelet packets and Hilbert–Huang transform. *Int J Mach Tools Manuf* 69:11–19
36. Fu Y, Zhang Y, Zhou H, Li D, Liu H, Qiao H, Wang X (2016) Timely online chatter detection in end milling process. *Mech Syst Signal Process* 75:668–688
37. Cao H, Zhou K, Chen X (2015) Chatter identification in end milling process based on EEMD and nonlinear dimensionless indicators. *Int J Mach Tools Manuf* 92:52–59
38. Daubechies I, Lu J, Wu H-T (2011) Synchrosqueezed wavelet transforms: an empirical mode decomposition-like tool. *Appl Comput Harmon Anal* 30(2):243–261
39. Yi-Hsin C, Yung-Hsin Y, Shu-Shya H, Chi-Tai K, Hau-Tieng W (2011) ECG-derived respiration and instantaneous frequency based on the synchrosqueezing transform: application to patients with atrial fibrillation. <https://arxiv.org/abs/1105.1571v1.pdf>
40. Thakur G, Brevdo E, Fučkar NS, Wu H-T (2013) The synchrosqueezing algorithm for time-varying spectral analysis: robustness properties and new paleoclimate applications. *Signal Process* 93(5):1079–1094
41. Wang P, Gao J, Wang Z (2014) Time-frequency analysis of seismic data using synchrosqueezing transform. *IEEE Geosci Remote S* 11(12):2042–2044
42. Li C, Liang M (2012) Time–frequency signal analysis for gearbox fault diagnosis using a generalized synchrosqueezing transform. *Mech Syst Signal Process* 26:205–217
43. Xi S, Cao H, Chen X, Zhang X, Jin X (2015) A frequency-shift synchrosqueezing method for instantaneous speed estimation of rotating machinery. *J Manuf Sci Eng* 137(3):031012
44. Cao H, Xi S, Chen X, Wang S (2016) Zoom synchrosqueezing transform and iterative demodulation: methods with application. *Mech Syst Signal Process* 72:695–711
45. Wang S, Chen X, Wang Y, Cai G, Ding B, Zhang X (2015) Nonlinear squeezing time–frequency transform for weak signal detection. *Signal Process* 113:195–210
46. van Dijk NJM, Doppenberg EJ, Faassen RPH, van de Wouw N, Oosterling JAJ, Nijmeijer H (2010) Automatic in-process chatter avoidance in the high-speed milling process. *ASME J Dyn Syst Meas Control* 132(3):031006